



**CHALMERS**  
UNIVERSITY OF TECHNOLOGY

---

# **Simulation Study on Lifted Hydrogen and Methane Jet Flames in Hot Vitiated Coflow**

Master's thesis in Automotive Engineering

HENRIK FORSTING



MASTER'S THESIS IN AUTOMOTIVE ENGINEERING

Simulation Study on Lifted Hydrogen and  
Methane Jet Flames in Hot Vitiated Coflow

HENRIK FORSTING

Department of Applied Mechanics  
CHALMERS UNIVERSITY OF TECHNOLOGY  
Gothenburg, Sweden 2017

Simulation Study on Lifted Hydrogen and Methane Jet Flames in Hot Vitiated Coflow  
HENRIK FORSTING

© HENRIK FORSTING, 2017

Master's thesis 2017:88  
Examiner: Michael Oevermann  
ISSN 1652-8557  
Department of Applied Mechanics  
Chalmers University of Technology  
SE-412 96 Gothenburg  
Sweden  
Telephone: +46(0)31-772 10000

Chalmers Reproservice  
Gothenburg, Sweden 2017

Simulation Study on Lifted Hydrogen and Methane Jet Flames in Hot Vitiated Coflow  
Master's thesis in Applied Mechanics  
HENRIK FORSTING  
Department of Applied Mechanics  
Chalmers University of Technology

## Abstract

Combustion of fossil fuels is the most important energy source today. Burning fossil fuel is however expensive and bad for the environment. Improving the combustion technology to reduce fuel consumption, and to be able to burn renewable fuels is therefore of great importance. Analysing the flames in gas turbine engine-like burners can give knowledge about the burning process, which can be used to improve the design of such engines, and to optimize their operating conditions. Simulations of a closed burner, used at Tongji University, have been conducted, where different operating conditions have been tested when burning hydrogen and methane.

For burning methane, different velocities of the jet and coflow have been simulated. For methane, the flame's liftoff height increased both when the jet- and the coflow velocity increased. The increase due to changes in coflow velocity was however smaller than the results from previous research on similar cases. When the jet velocity was between 25 to 75 m/s, the flame's liftoff height was very dependent on the coflow velocity. At speeds ranging from 75 to 200 m/s, the liftoff height was less dependent of coflow velocity. The jet's reduced influence was due to a recirculating zone that appeared at high jet velocities. A jet velocity of 50-100 m/s gives a liftoff height that is neither too low, nor too high, and no recirculating zone is formed in those jet velocities.

For hydrogen, different jet velocities and background pressures have been simulated. For the hydrogen case, the flame was blown out at fairly low pressures. The flame was blown out as early as 1.2 bar when the jet velocity was set to 107 m/s. The pressure limit rose as the jet velocity declined, and with a jet velocity of 25 m/s, the limit was logged to 1.4 bar. There is no clear trend for the liftoff behaviour from 1.0 to 1.1 bar, but the liftoff height increase rapidly when the pressure increase beyond 1.1 bar. When using hydrogen as a fuel, the pressure must be controlled very precisely to be able to run it efficiently, due to the flames sensibility to pressure differences.

**Keywords:** Lifted Flames, Coflow, Jet, Liftoff Height, Blow Out, Closed Burner, Internal Combustion, Simulation



## Acknowledgement

I would like to express my deepest gratitude to my peers at my research team for letting me be part of their research. I especially want to thank Qing Zhang and Wei Xie for their invaluable assistance throughout the project. Without your help, my simulations would still be running.

My sincere thanks also go to my examiner Professor Michael Oevermann for his patience and precious feedback during the project.

I would also like to thank the School of Automotive Studies at Tongji University for giving me the great opportunity to conduct my research at their fine University. Thank you for this golden opportunity to investigate an interesting technology, and to do so in a true international environment.

Last but not least, I would like to thank the Automotive Engineering programme at Chalmers University of Technology for making it possible to do the research in China.



# Nomenclature

## Upper Case Roman Letters

$C_{1\varepsilon}$	Constant: 1.44
$C_{2\varepsilon}$	Constant: 1.92
$C_{3\varepsilon}$	Constant: -0.33
$C_\mu$	Constant: 0.09
$C_\phi$	Mixing constant: 2
$G_b$	Generation of turbulence kinetic energy due to buoyancy
$G_k$	Generation of turbulence kinetic energy due to the mean velocity gradients
$H$	Liftoff height
$J_{i,k}$	Molecular diffusion flux vector
$K$	Kelvin
$L$	Characteristic length
$N$	Total number of particles in the cell
$P$	Favre joint PDF of composition
$Re$	Reynolds number
$S_\varepsilon$	User-defined source term
$S_K$	User-defined source term
$S_k$	Reaction rate for species $k$
$Sc_t$	Turbulent Schmidt number
$T$	Temperature
$V$	Velocity
$V_{coflow}$	Coflow velocity
$V_{jet}$	Jet velocity
$X$	Mole fraction
$Y_M$	The contribution of the fluctuating dilatation in compressible turbulence to the overall dissipation rate
$Y_{OH}$	Mass fraction of hydroxide

### Lower Case Roman Letters

$d$	Nozzle diameter
$f$	Mixture fraction
$f_s$	Stoichiometric mixture fraction
$k$	Turbulence kinetic energy
$m$	Metre
$m_a$	Mass of air
$m_f$	Mass of fuel
$m_i$	Mass of particle $i$
$m_j$	Mass of particle $j$
$s$	Second
$u_i$	Favre mean fluid velocity vector
$u_i^n$	Fluid velocity fluctuation vector
$z$	Liftoff height

### Abbreviations

CFD	Computational Fluid Dynamics
EMST	Euclidean Minimum Spanning Tree
PDF	Probability Density Function

### Greek Letters

$\varepsilon$	Rate of dissipation
$K$	Eddy diffusivity
$\mu$	Dynamic viscosity
$\mu_t$	Turbulent viscosity
$\mu_t$	Turbulent viscosity
$\nu$	Kinematic viscosity
$\nu_t$	Eddy viscosity
$\xi$	A uniform random number
$\rho$	Density
$\sigma_k$	Turbulent Prandtl number for $k$

$\sigma_\varepsilon$	Turbulent Prandtl number for $\varepsilon$
$\tau_t$	Turbulent time scale
$\phi$	Equivalence ratio
$\phi_i$	Composition vector of particles $i$
$\phi_j$	Composition vector of particles $j$
$\psi$	Composition space vector

# Contents

ABSTRACT .....	I
ACKNOWLEDGEMENT .....	III
NOMENCLATURE.....	V
CONTENTS.....	VIII
1. INTRODUCTION .....	1
2. THEORY.....	3
2.1. TURBULENCE.....	3
2.1.1 <i>The standard k-ε model</i> .....	3
2.2. COMBUSTION.....	4
2.2.1 <i>Premixed combustion</i> .....	4
2.2.2 <i>Non-premixed combustion</i> .....	4
2.3. FLAME STABILIZATION.....	5
2.4. CHEMISTRY MODELS .....	5
2.4.1 <i>The Composition PDF Transport Model</i> .....	6
2.4.2 <i>The Modified Curl Model</i> .....	7
2.5. RADIATION .....	8
3. PREVIOUS FINDINGS .....	9
4. METHODOLOGY AND SETUP .....	14
4.1. APPROACH.....	14
4.2. SOFTWARE.....	14
4.3. MODEL OF THE BURNER .....	14
4.3.1 <i>Geometry</i> .....	14
4.3.2 <i>Mesh</i> .....	15
4.4. SETUP .....	16
4.4.1 <i>Boundary Conditions</i> .....	16
4.4.2 <i>Models</i> .....	17
5. RESULTS.....	19
5.1. METHANE.....	19
5.1.1 <i>Coflow velocity</i> .....	19
5.1.2 <i>Jet Velocity</i> .....	20
5.2. HYDROGEN .....	23
6. DISCUSSION .....	26
6.1. RELEVANCE TO THE AUTOMOTIVE INDUSTRY.....	27
7. CONCLUSION .....	28
8. RECOMMENDATIONS AND SUGGESTIONS FOR FURTHER WORK .....	28
9. BIBLIOGRAPHY.....	29
APPENDIX.....	31

# 1. Introduction

Combustion of fossil fuels is the most important energy source in the world today. The world economy is heavily dependent on fossil fuels, and many sectors, especially the heavy industry and the transport sector, have no cheap substitutes to fossil fuels. There are however several problems with fossil fuels: It is a non-renewable energy source, so the production will someday inevitably decrease, so there will eventually be no other choice than to use other energy sources. Combustion of fossil fuels accumulate carbon dioxide in the atmosphere which lead to a rising global temperature and acidification of the oceans. The consequences are hard to predict in details, but they will generally be bad for humans. The combustion also lead to other products that are released to the atmosphere that are bad for humans, such as  $\text{NO}_x$  and soot. There is also a political risk with fossil fuels since basically all countries are dependent on the source, but the majority of the supply comes only from a few countries, many of which being non-democracies.

The problems mentioned above makes it desirable to improve the use of fossil fuels and to substitute it with other energy sources. One way to improve the use of fossil fuels is simply to make the combustion of it more efficient by fine tuning the engines. Another way to deal with some of the problems is to convert fossil fuels to hydrogen by gasification. Gasification is the process of converting fossil fuels to carbon monoxide, carbon dioxide and hydrogen. Engines, like the gas turbine, can run on hydrogen and they will have zero emissions of carbon dioxide. The gasification does however produce carbon dioxide, but since the conversion is on an industrial scale, it is possible to implement carbon capturing and storage techniques to make sure that no new carbon dioxide is added to the atmosphere.

Introducing hydrogen as a fuel to turbine engines has been a challenge for researchers. There are significant differences in the combustion process when burning hydrogen compared to burning conventional fossil fuels. Stabilizing the flame has proven to be one of the difficulties.

Previous research on the combustion in turbine engines has been through both laboratory experiments and computer simulations. The improvements in the physics models, combined with the improvements in computational power, have made simulations both trustworthy, fast, and cheap. This improvement in technology has made research based on computational fluid dynamics (CFD) more popular over the last years. Physical experiments are however still very important too.

The approach of the research in this report is based solely on CFD simulations. The computer model is based on the burner used at the School of Automotive Studies at Tongji University in Shanghai. Figure 1 shows a simplified design of the chamber. The fuels used are methane and hydrogen. This report presents an investigation of how the combustion, mainly the flame and its liftoff height, behave under different conditions. The parameters being changed in the different conditions are coaxial flow (coflow) velocity, jet velocity, and background pressures. The report also tries to explain the phenomena behind the observations. A better understanding of the flames will help improving the efficiency in turbine engines.

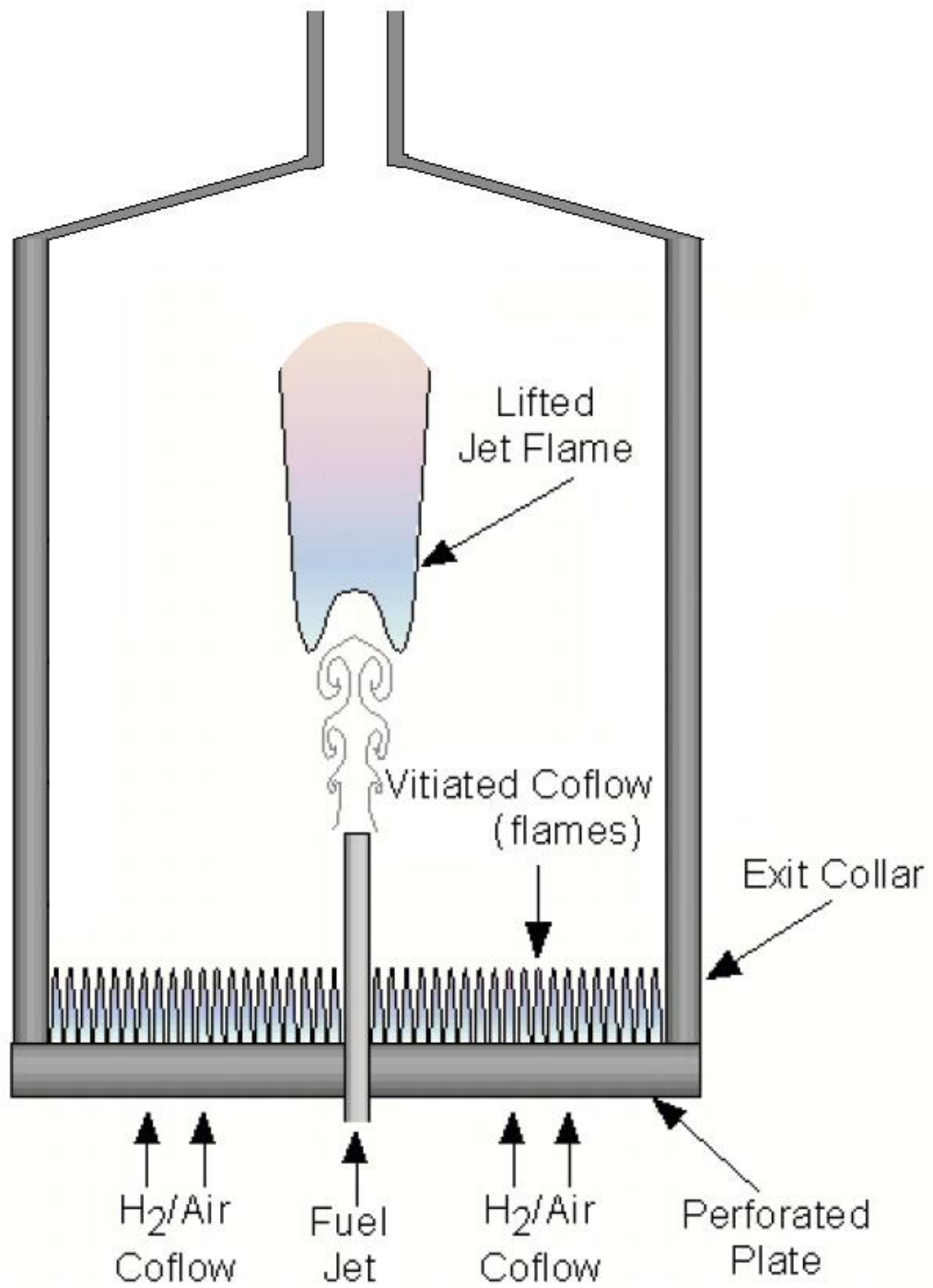


Figure 1. Lifted jet flame in coaxial flow.

## 2. Theory

This section presents the most important theories for describing the relevant physics in the burner and in the different computer models that has been used. There are lots of different models that are used in CFD, and they all have their advantages and disadvantages. Some models have proven to be accurate for some scenarios, and less accurate in other scenarios. The models described here are the ones that have been used in the simulations in this project

### 2.1. Turbulence

Turbulent flows are common in both nature and technology, and it can easily be observed in rivers and chimneys. Turbulence plays a part in big geophysical phenomenon like hurricanes, and it is also present in smaller scale, e.g. in pipes and nozzles. Even though turbulence is common and thoroughly researched, there is no universally adopted definition of the phenomenon (Lumley, 1990). However, descriptions of turbulence often highlight the three dimensional chaotic behaviour where pressure and velocity is continuously changing, the presence of eddies stretching from sizes down to molecular level up to the size of the whole system, and that it is strongly dissipative and diffusive (Westerweel, Boersma, Nieuwstadt, 2016). Turbulent flow generally occurs at Reynolds numbers,  $Re$ , above 5000. Reynolds number is defined as

$$Re = \frac{\rho VL}{\mu} = \frac{VL}{\nu} \quad (\text{Equation 1})$$

where  $\rho$  is density,  $V$  is the velocity of the fluid,  $L$  is characteristic length,  $\mu$  is dynamic viscosity, and  $\nu$  is the kinematic viscosity (White, 2011).

#### 2.1.1 The standard $k$ - $\varepsilon$ model

The standard  $k$ - $\varepsilon$  model is a two transport equation turbulence model that is able to determine both time scale and turbulent length. Although it is a simplification of reality, the model's accuracy and time efficiency has made it widely used in computer simulations that are similar to those that are presented in this report.

The transport equations that are solved to obtain the turbulence kinetic energy,  $k$ , and its rate of dissipation,  $\varepsilon$ , are

$$\frac{\partial}{\partial t}(\rho k) + \frac{\partial}{\partial x_i}(\rho k u_i) = \frac{\partial}{\partial x_j} \left[ \left( \mu + \frac{\mu_t}{\sigma_k} \right) \frac{\partial k}{\partial x_j} \right] + G_k + G_{kb} - \rho \varepsilon - Y_M + S_K \quad (\text{Equation 2})$$

and

$$\frac{\partial}{\partial t}(\rho \varepsilon) + \frac{\partial}{\partial x_i}(\rho \varepsilon u_i) = \frac{\partial}{\partial x_j} \left[ \left( \mu + \frac{\mu_t}{\sigma_\varepsilon} \right) \frac{\partial \varepsilon}{\partial x_j} \right] + C_{1\varepsilon} \frac{\varepsilon}{k} (G_k + C_{3\varepsilon} G_b) - C_{2\varepsilon} \rho \frac{\varepsilon^2}{k} + S_\varepsilon \quad (\text{Equation 3})$$

Where  $G_k$  represents the generation of turbulence kinetic energy due to the mean velocity gradients,  $G_b$  is the generation of turbulence kinetic energy due to buoyancy,  $Y_M$  represents the contribution of the fluctuating dilatation in compressible turbulence to the overall dissipation rate.  $C_{1\varepsilon}$ ,  $C_{2\varepsilon}$ , and  $C_{3\varepsilon}$  are constants.  $\sigma_k$  and  $\sigma_\varepsilon$  are the turbulent Prandtl numbers for  $k$  and  $\varepsilon$ , respectively.  $S_K$  and  $S_\varepsilon$  are user-defined source terms. (Ansys, 2006)

$\mu_t$  is the turbulent viscosity, and it is calculated by combining  $k$  and  $\varepsilon$  as

$$\mu_t = \rho C_\mu \frac{k^2}{\varepsilon} \quad (\text{Equation 4})$$

where  $C_\mu$  is a constant.

The constants values are

$$C_{1\varepsilon} = 1.44, C_{2\varepsilon} = 1.92, C_{3\varepsilon} = -0.33, C_{\mu} = 0.09, \sigma_k = 1.0, \text{ and } \sigma_{\varepsilon} = 1.3$$

Assumptions in the derivation of this model are that the flow is fully turbulent and that the molecular viscosity effects are insignificant, hence the model is only valid for fully turbulent flows. (Ansys, 2006)

## 2.2. Combustion

Combustion is the process of an exothermic chemical reaction between a fuel and an oxidant. The oxidant is often the oxygen from air, and the fuel can be wood, oil, coal, or gas to mention a few of the common ones. Combustion requires the fuel and the oxidizer to be mixed on a molecular level in combination with a high enough temperature.

There are two main categories of flames based on how the fuel and oxidizer molecules are mixed. The mixture can either be mixed before the combustion starts, called premixed flames, or it can mix simultaneously as the combustion takes place, called non-premixed flames. These categories can be further divided based on if the flame is laminar or turbulent. (Warnatz, 2006)

### 2.2.1. Premixed combustion

Turbulent premixed flames are found in various devices such as the spark-ignited gasoline engine and gas turbines. In the premixed combustion, the fuel and oxidizer are mixed before ignition occurs. The chemistry in the premixed flame evolves quickly from unburnt to burnt at the interface between reactants and the products. The propagation of the interface is denoted as the flame speed (Warnatz, 2006).

A popular measurement of the mixtures composition of fuel and oxidizer is the equivalence ratio,  $\phi$ , which is the normalized actual fuel-air ratio by the stoichiometric fuel-air ratio.  $\phi$  is defined as

$$\phi = \frac{f}{f_s} \quad (\text{Equation 5})$$

where

$$f = \frac{m_f}{m_a} \quad (\text{Equation 6})$$

and

$$f_s = \left. \frac{m_f}{m_a} \right|_{\text{stoichiometric}} \quad (\text{Equation 7})$$

where  $m_f$  and  $m_a$  are the respective masses of the fuel and air (McAllister, Chen, Fernandez-Pello, 2011).  $\phi < 1$  is a lean mixture,  $\phi = 1$  is a stoichiometric mixture, and  $\phi > 1$  is a rich mixture.  $\phi$  is bounded by 0 and  $\infty$ , which corresponds to pure air and fuel respectively (ibid.).

### 2.2.2. Non-premixed combustion

In non-premixed combustion, the mixing of fuel and oxidizer occurs during the combustion process. In non-premixed combustion, the equivalence ratio range from 0 to  $\infty$ , and rich and lean combustion is taking place simultaneously. The chemistry is therefore more complex when the gases are non-premixed compared to when they are premixed. Under some circumstances it is however not always clear if the combustion is non-premixed or premixed. For example, when local flame extinction in a non-premixed flame occurs, it allows fuel and air to mix before being ignited by an adjacent non-premixed flame zone. The flame is brightest near the region where the equivalence is close to 1, since that is where the temperature is the highest. Since the combustion takes place as the gases mixes, the flame cannot propagate, hence it does not have a flame speed. The flame is often yellow due to

glowing soot formed locally, where the combustion is rich. The soot problem is possible to get around, but it requires very sophisticated mixing techniques. (Warnatz, 2006)

### 2.3. Flame stabilization

Flame stabilization is of fundamental importance to turbulent combustion design. Being able to have a stable flame is a key factor for being able to operate the process safely, efficiently and with control over the emissions. A flame is stable when it is anchored at a chosen location and when it is resistant to flashback, liftoff and blowout over the operating range of the device (Turns, 2006).

A flame attached to the hot nozzle rim is the simplest case of a stabilized flame. This simple case is however not common in industrial burners since the jet velocity is too high. Attached flames are also unwanted in some designs since they can damage the burner's nozzle (Mansour, 2003). When the jet velocity is too high to support attached flow, the flame will lift off and it will stabilize downstream of the nozzle. There are various mechanisms that influence the liftoff height. Two of these are dominating and work in opposite directions: flame quenching by turbulence leads to liftoff, and premixed flame propagation work in the opposite direction (Navarro-Martinez & Kronenburg, 2011). Navarro-Martinez and Kronenburg (2011) also argues that auto-ignition of the mixture, made possible by hot coflow or product gases, might be a mechanism that is so influential that it makes the liftoff height largely independent of flame propagation. Experiments show that the liftoff height is very sensitive to coflow temperature both when methane and hydrogen are used as fuel. However, when simulating the auto-ignition process, detailed chemical models are required since it is very sensitive to radical formation (ibid).

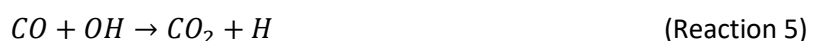
Although flame stabilization for lifted flames has been under research for many years, there is no satisfactorily theoretical explanation for the mechanisms when it comes to turbulent flames (Tacke, Geyer, Hassel & Janicka, 1998; Leung & Wierzbka, 2009). Models that only aim to predict the behaviour of the liftoff height of the flame have been suggested, but they have not been able to show consistency when tested in experiments (Cabra, Chen, Dibble, Karpetis & Barlow, 2005). The approach to research liftoff flames has mainly been to draw conclusions based on laboratory experiments and simulations.

### 2.4. Chemistry Models

Chemical reactions are a lot more complex than often being depicted in school books. The chemical reactions are usually described as going straight from state A to state B. Burning methane is a common example of a chemical reaction. When seen in textbooks, it will often be described as



This description is often a good enough explanation for many practical problems, but when studying the characteristics of a burning flame, the model is too simple, so the calculations will differ substantially from reality. In reality, chemical reactions take place over many steps, sometimes hundreds of steps. Some of the steps involved in Reaction 1 are



just to mention a few. Not only is it important to capture what steps the reaction takes, physical parameters such as heat release and specific heat capacity are also important to take into

consideration. To be able to simulate the reality in an acceptable manner, it is crucial to capture at least the most important reactions. As always when it comes to simulations, the more detailed the models, the more accurate the results will be, but also more time consuming. There are ways to simulate chemical reactions in detail efficiently, one way is to use the composition probability density function transport model.

#### 2.4.1. The Composition PDF Transport Model

By applying probability density functions (PDF) when modelling chemical kinetic effects in turbulent reacting flows, it is possible to tackle problems that are otherwise hard to solve. PDF methods treat convection and finite rate non-linear chemistry exactly, they are therefore highly capable of modelling turbulent flames. Molecular mixing is the only effect that has to be modelled. (Senouci, Benchatti, Bounif, Oumrani, Merouane, 2016)

One of these models is the composition PDF transport model. This model, integrated within a conventional CFD, is an efficient tool when studying turbulent combustion (Senouci et al., 2016). Although the model is efficient, it still requires a lot of computational power. It is therefore recommended to keep the meshes small and to preferably work in 2D (Ansys, 2006).

Ansys' (2006) interpretation of PDF: "This PDF, denoted by  $P$ , can be considered to represent the fraction of the time that the fluid spends at each species, temperature and pressure state."  $P$  has one dimension for each species, denoted  $N$ , plus one dimension for temperature and one dimension for pressure spaces. Hence,  $P$  has  $N + 2$  dimensions. Any single-point thermos-chemical moment can be calculated using the PDF (Ansys, 2006). The PDF transport equation is derived from the Navier-Stokes equation as (Ansys, 2006):

$$\frac{\partial}{\partial t}(\rho P) + \frac{\partial}{\partial x_i}(\rho u_i P) + \frac{\partial}{\partial \psi_k}(\rho S_k P) = -\frac{\partial}{\partial x_i}[\rho \langle u_i^n | \psi \rangle P] + \frac{\partial}{\partial \psi_k} \left[ \rho \left\langle \frac{1}{\rho} \frac{\partial J_{i,k}}{\partial x_i} \middle| \psi \right\rangle P \right] \quad (\text{Equation 8})$$

where

$P$ = Favre joint PDF of composition

$\rho$ = mean density of fluid

$u_i$ = Favre mean fluid velocity vector

$S_k$ = reaction rate for species  $k$

$\psi$ = composition space vector

$u_i^n$ = fluid velocity fluctuation vector

$J_{i,k}$ = molecular diffusion flux vector

The first term on the left hand side of Equation 8 is the unsteady rate of change of the PDF, the second term is the change of the PDF due to convection by the mean velocity field, and the third term is the change due to chemical reactions. All the terms on the left hand side are highly nonlinear, but they are also closed, hence they do not have to be modelled, which is the principal strength of the PDF transport approach. The two terms on the right hand side are however not closed, and they have to be modelled. The first term on the right hand side represent the PDF change due to scalar convection by turbulence (turbulent scalar flux), the second term represent the molecular mixing and diffusion. (Ansys, 2006)

The turbulent scalar flux is modelled in Ansys by the gradient-diffusion assumption (Ansys, 2006):

$$-\frac{\partial}{\partial x_i} [\rho \langle u_i^n | \psi \rangle P] = \frac{\partial}{\partial x_i} \left( \frac{\rho \mu_t}{Sc_t} \frac{\partial P}{\partial x_i} \right) \quad (\text{Equation 9})$$

where  $\mu_t$  is the turbulent viscosity, which is calculated in the turbulence model. The standard  $k$ - $\epsilon$  model uses Equation 4 to determine  $\mu_t$ .  $Sc_t$  is the turbulent Schmidt number, defined as

$$Sc_t = \frac{\nu_t}{K} \quad (\text{Equation 10})$$

where  $\nu_t$  is the eddy viscosity and  $K$  is the eddy diffusivity.

#### 2.4.2. The Modified Curl Model

The last term of Equation 8 represent, as mentioned, the molecular mixing. Combustion takes place at the smallest molecular scale, so being able to model the mixing adequately is crucial to obtain realistic results. Modelling the mixing process is not straightforward, and it is usually the source of the largest modelling error in the PDF transport approach (Ansys, 2006). There are several mixing models and one of the most popular models used by researchers working on similar problems as the one presented in this paper is the modified curl model (sometimes called the m-curl model). The model randomly selects a few particle pairs per cell, and their individual compositions are moved towards their mean composition. The number of pairs being selected is very complicated and it requires a long and complex algorithm which is too long to describe here. The algorithm can solve for any general case, but in the special case for pairs with particles of equal mass, there is a short cut (Ansys, 2006):

$$N_{pair} = \frac{1.5C_\phi N \Delta t}{\tau_t} \quad (\text{Equation 11})$$

where

$N$ = total number of particles in the cell

$C_\phi$ = mixing constant (Ansys use 2 by default)

$\tau_t$ = trubulent time scale (for the standard  $k$ - $\epsilon$  model this is  $k/\epsilon$ )

A uniform random number,  $\xi$ , is designated for each particle pair, and each particle's composition,  $\phi$ , is moved towards the pair's mean composition by a factor proportional to  $\xi$  (Ansys, 2006):

$$\phi_i^1 = (1 - \xi)\phi_i^0 + \xi \frac{(\phi_i^0 m_i + \phi_j^0 m_j)}{(m_i + m_j)} \quad (\text{Equation 12})$$

$$\phi_j^1 = (1 - \xi)\phi_j^0 + \xi \frac{(\phi_i^0 m_i + \phi_j^0 m_j)}{(m_i + m_j)} \quad (\text{Equation 13})$$

where  $\phi_i$ , and  $\phi_j$  are the composition vectors of particles  $i$  and  $j$ , and  $m_i$  and  $m_j$  are the masses of particles  $i$  and  $j$  respectively.

One of the main flaws of the modified curl model is that the particles are not continuously filling up the space, so the locations of the particles are spread out with gaps of space between them. The consequence can lead to inert mixing over reaction zones, which is not in line with the actual behaviour of the gases. There are models that do not suffer from this problem, e.g. the Euclidean minimum spanning tree model (commonly only referred as the EMST model). This model does however have its

downsides as well, one of them being its computational cost, which is proportional to the square of the number of particles per cell. In conclusion: none of the models are perfect, but the modified curl model is usually considered as one of the better and therefore often used in PDF simulations (Meyer & Jenny, 2013)

## 2.5. Radiation

Heat is transferred by thermal conduction, thermal convection, thermal radiation, and phase transition. Of these, phase transition is the only heat transfer that is not present in the chamber. The temperature is always too hot for the gas to condensate, yet too low to ionise. Out of the three remaining mechanisms, conduction and convection are the simplest to simulate. There are no options to be made in Ansys when deciding to include conduction and convection, so those two will not be presented here. Since radiation, on the other hand, is complex, Ansys gives a variety of models to choose from, each of which with their specific advantages and disadvantages (Ansys, 2006).

The model that is the most popular to use among researchers who work with similar burners as in this project is the P-1 radiation model. The P-1 radiation model is the simplest case of the general P-N radiation model. The main advantage of the P-1 model is that it is very fast (Krishnamoorthy, 2017). Its main disadvantages are that it works poorly with optically thin media, and the model assumes that all surfaces are completely diffuse (Krishnamoorthy, 2017; Ansys 2006). Despite these disadvantages, the P-1 has been reported to work well. The shortcomings are sometimes influencing the results, but overall the errors are acceptable (Cintolesi, Nilsson, Petronio & Armenio, 2017).

As mentioned, the model is very complex, so the equations will not be presented here but they can be found in Ansys' user guide (2006). It is important to emphasise that the heat transfer due to radiation is small. Many researchers working on burners simply ignore radiation all together in their simulations, so including a radiation model in the simulations can be expected to have minor impacts on the final results of the simulations.

### 3. Previous Findings

Previous research of the characteristics of lifted flames in hot coflow has been carried out with both laboratory experiments and computer simulations. This section presents the findings of the previous research. A comparison between the findings of this report and of previous research is found under *Results and Discussion*.

There have not yet been any laboratory experimental results published from a burner with the same dimensions and with the same boundary conditions used in this paper, so there are no results available to directly compare with. The previous findings that are presented are however from experiments that are similar to the ones carried out in this study, so general trends and phenomenon should reasonably be relatively similar, which makes them relevant to compare with.

Cabra et. al. (2005) have investigated how coflow- and jet velocity affect the liftoff height of the flame. Their set up and boundary conditions were similar to the ones used here, but the biggest difference is that they used an open chamber instead of a closed one. Measurements of the diameter of the jet nozzle is the same, the chemical compositions differ with just a few per mille units, and the coflow- and jet velocities are the same. Table 1 shows the boundary conditions used in the base-conditions in the paper by Cabra et. al. (2005).

Table 1. Base-case conditions for the vitiated coflow burner. Conditions for both the hydrogen and the methane cases are listed.  $X$ , mole fraction;  $Re$ , Reynolds number;  $d$ , nozzle diameter;  $\phi$ , equivalence ratio;  $f_s$ , stoichiometric mixture fraction;  $V$ , velocity;  $T$ , temperature. (Cabra et. al., 2005)

Base-case conditions for the vitiated coflow burner				
	Hydrogen		Methane	
	Jet	Coflow	Jet	Coflow
$Re$	23,600	18,600	28,000	23,300
$d$ (mm)	4.57	210	4.57	210
$V$ (m/s)	107	3.5	100	5.4
$T$ (K)	305	1,045	320	1,350
$X_{O_2}$	0.0021	0.15	0.15	0.12
$X_{N_2}$	0.74	0.75	0.52	0.73
$X_{H_2O}$	0.0015	0.099	0.0029	0.15
$X_{OH}$ (ppm)	<1	<1	<1	200
$X_{H_2}$	0.25	$5 \times 10^{-4}$	100	100
$X_{NO}$ (ppm)	–	–	<1	<1
$X_{CH_4}$	–	–	0.33	0.0003
$\phi$	–	0.25	–	0.4
$f_s$		0.473		0.177

Figure 2 and Figure 3 show how the liftoff height of the flame changes with different coflow- and jet velocities in laboratory experiments as well as when calculated (Carba et. al., 2005).  $H$  is the liftoff height and  $d$  is the nozzle diameter. The plots show that the simulations follow the same general trends as the experiments: when the jet velocity increase, so does the liftoff height. The same goes for coflow velocity. The simulations predicts how the liftoff height changes with respect to jet velocity quite accurately, but the prediction of change with respect to coflow velocity is underestimating the relationship. The authors suggest that this might be due to inherent assumptions in the underlying models, but they stress that they do not know for sure.

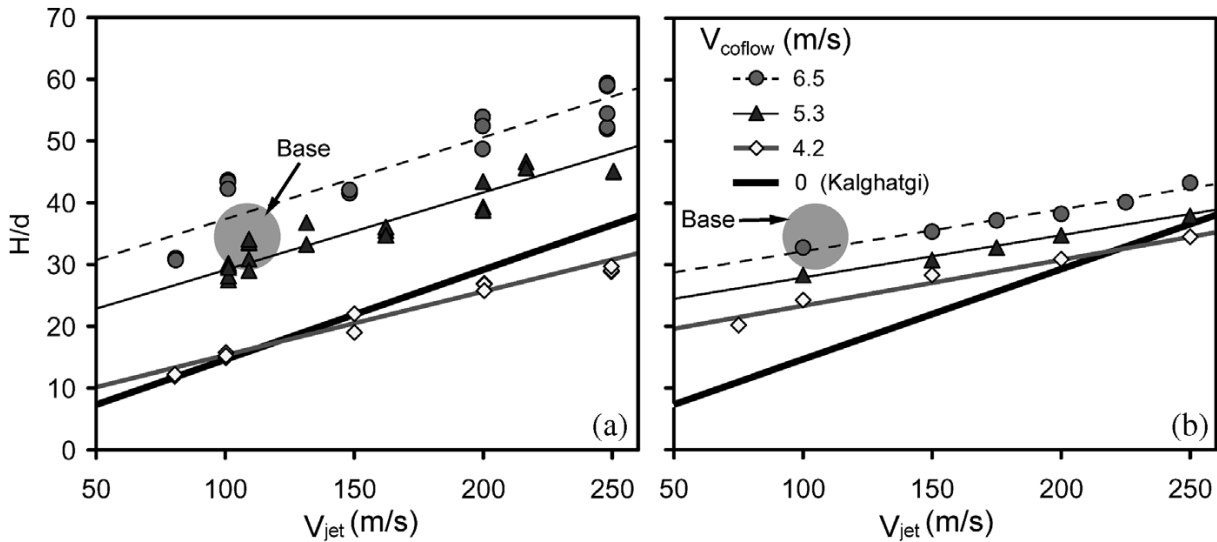


Figure 2. Sensitivity of CH4/air flame liftoff height to jet exit velocity, with coflow velocity as a parameter. The shaded circle represents the base-case liftoff height established by the unaided eye. Plotted are the experimental results (a) and the PDF with M-Curl mixing results (b). The thick line shows the prediction from Kalghatgi's correlation.  $H/d$  is height divided by nozzle diameter. (Carba et. al., 2005)

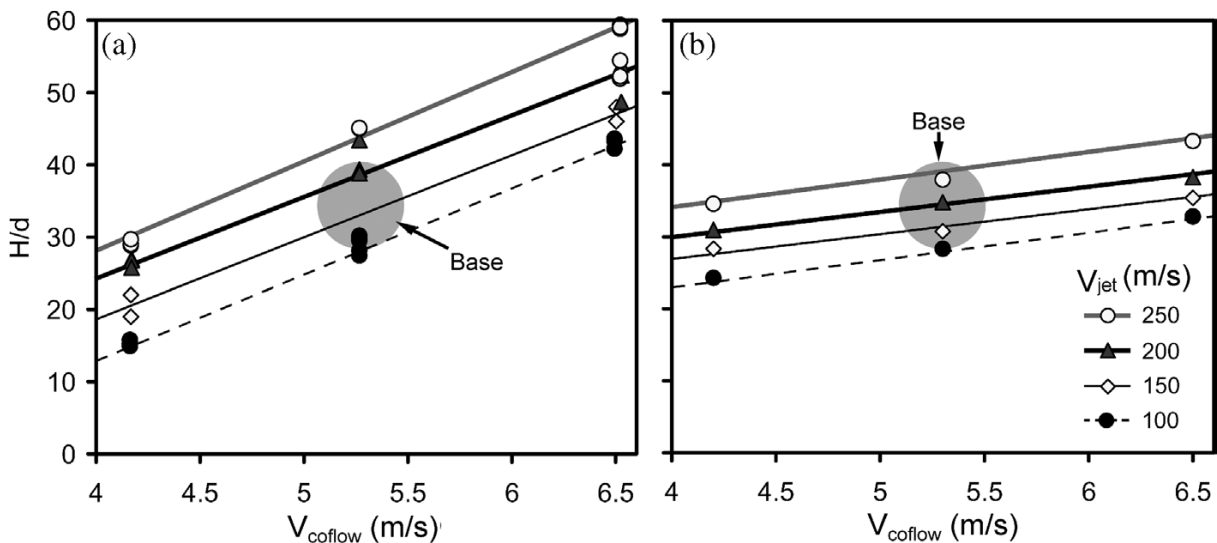


Figure 3 Sensitivity of CH4/air flame liftoff height to coflow velocity, with jet exit velocity as a parameter. The shaded circle represents the base-case liftoff height established by the unaided eye. Plotted are the experimental results (a) and the PDF with M-Curl mixing results (b).  $H/d$  is height divided by nozzle diameter. (The same data as in Figure 2 is used here.) (Carba et. al., 2005)

Cabra et al. (2005) present data of the OH mole fraction at four axial stations in both the lifted methane- and hydrogen flame from experiments, shown in Figure 4 and Figure 5 respectively. The figures show the transition from a non-reacting flow (pure mixing) to a reacting flow. One of the most notable differences from the figures is that the flame stabilizes much closer to the nozzle for hydrogen compared to methane. The liftoff height for the methane is around 35  $z/d$  (liftoff height divided by nozzle diameter), but only around 10  $z/d$  for hydrogen. The plots where the temperature of the HO-mixture fraction lies between the equilibrium line and the pure mixing lines indicates that the flame is unstable in those regions. As can be seen, the flames fluctuates for both fuels, and the fluctuations takes place over a vertically distance of many times the nozzle diameter. However, the fluctuations are not equally large, they are proportionally smaller for hydrogen compared to methane. (Cabra et al, 2005)

From the diagrams it is also notable that all chemical kinetic activity occurs where the mixture fraction is below 0.4. These regions are associated with lower velocities, lower turbulence intensities, and higher temperatures, hence the coflow conditions should have greater influence of the combustions processes of the lifted jet flame compared to the jet conditions. The data presented in Figure 2 and Figure 3 confirm this belief. (Cabra et al, 2005)

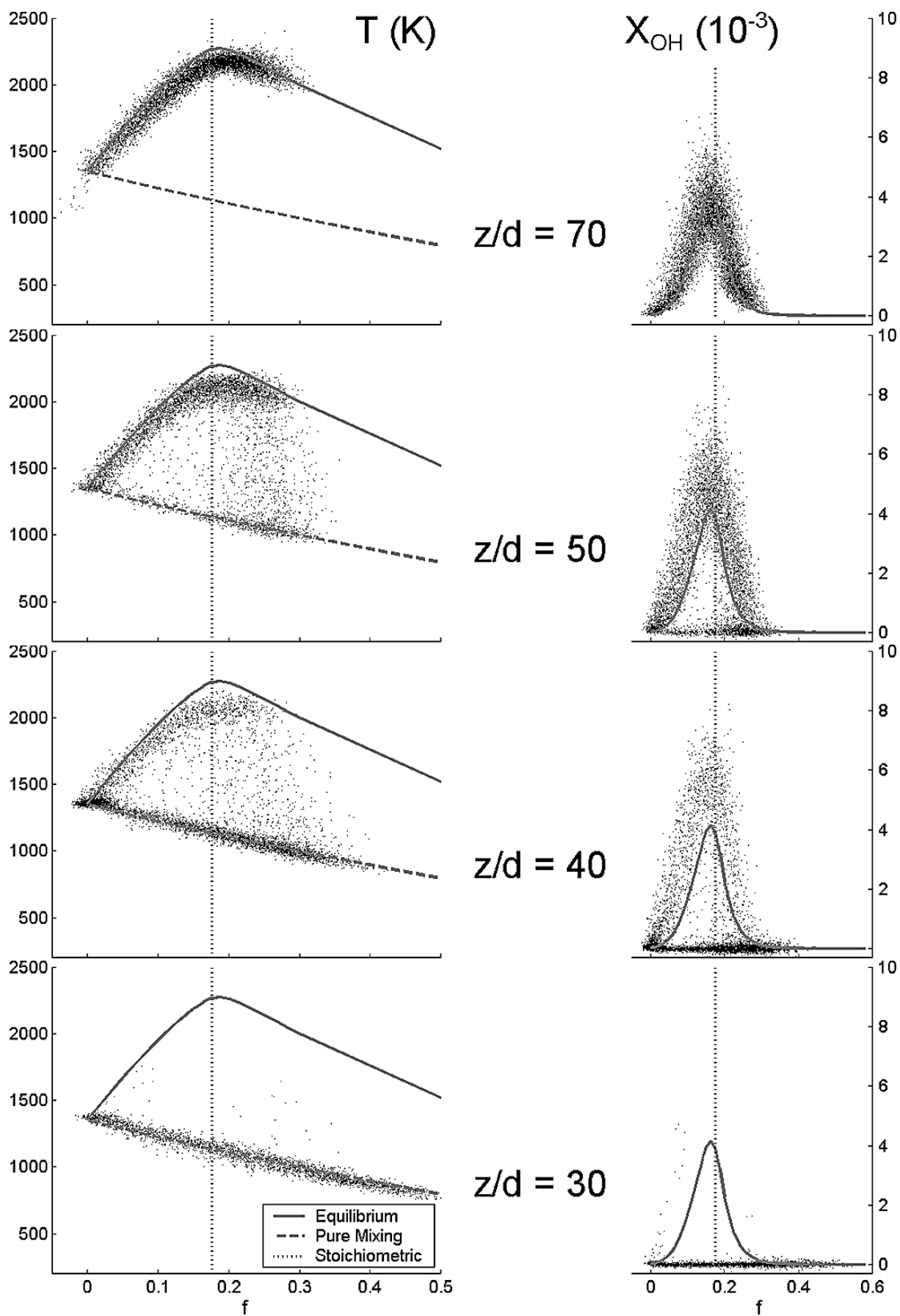


Figure 4. Distributions of instantaneous temperature and OH mole fraction at four axial stations in the lifted CH<sub>4</sub>/air flame.  $z/d$  is height divided by nozzle diameter and  $f$  is mixture fraction. (Carba et. al., 2005)

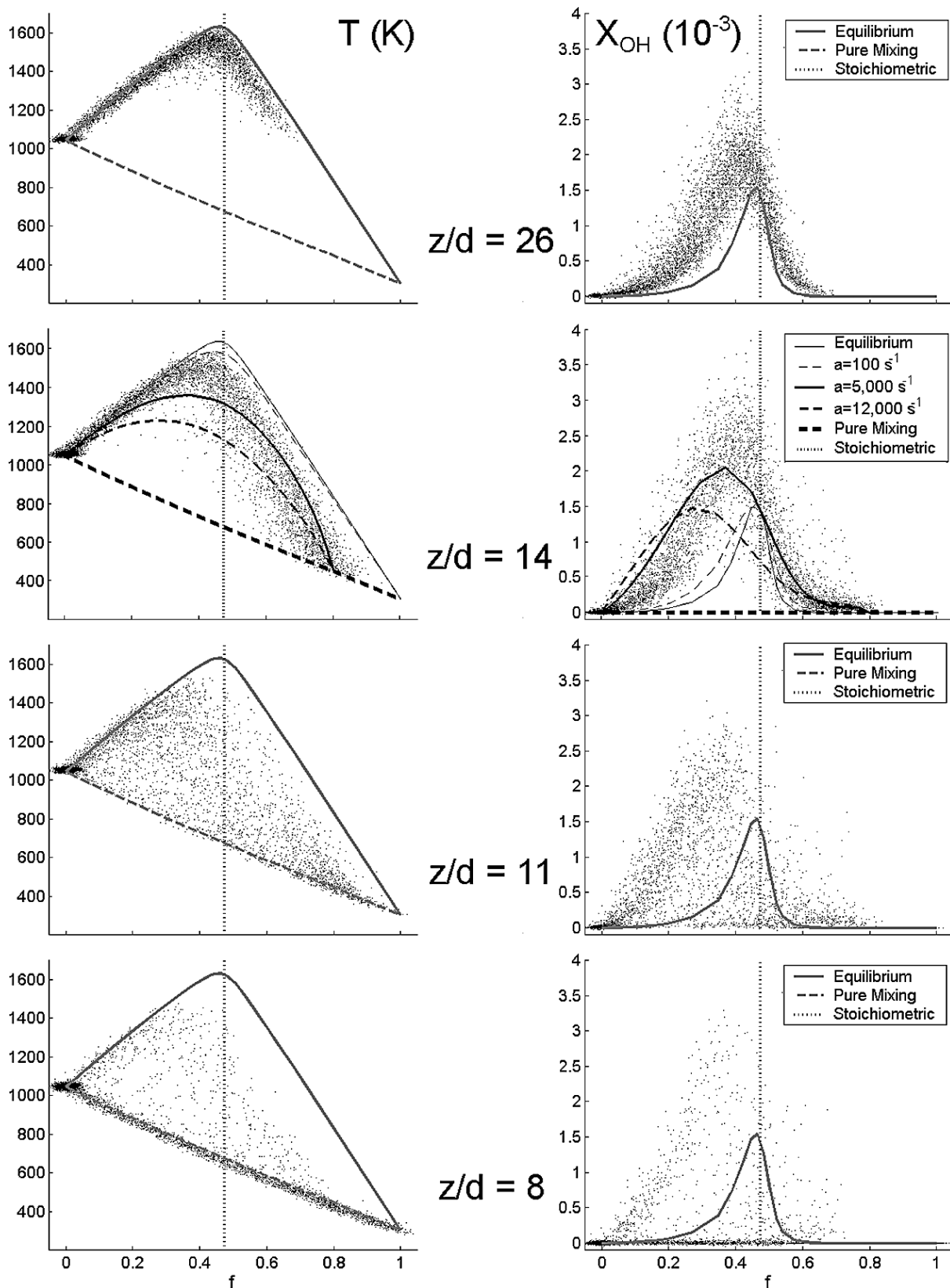


Figure 5. Distributions of instantaneous temperature and OH mole fraction at four axial stations in the lifted H<sub>2</sub>/N<sub>2</sub> flame.  $z/d$  is height divided by nozzle diameter and  $f$  is mixture fraction. (Carba et. al., 2002)

## 4. Methodology and Setup

In this section the methodology will be presented. Approach, software, settings, and physical models used will be described.

### 4.1. Approach

There are two approaches when it comes to investigating the behaviour of the flame: laboratory experiments, and computational simulations. In previous research, both approaches are popular. The general trend is however that the popularity of simulations are growing. The processing power of computers grow exponentially, and the consumer price of processing power falls. This makes it possible to simulate complex processes, like fluid mechanics, in a reasonable amount of time and to a low investment cost in hardware. One of the main advantages of using computers is that it is easy to control and it is easy to make changes in the model and in the boundary conditions. Rebuilding the geometry in physical prototypes are often very costly and time consuming, but changing the geometries in the computer is both relatively fast and easy. Changing boundary conditions like pressure or inlet velocity can be made within a few seconds. Another great advantage of simulations is that it is easy to obtain the data of the results. (Wilcox, 2006)

The physics behind the behaviour of flowing and burning gases is very complex. The equations that describe the physics are more or less impossible to solve analytically. Scientists have not been able to completely understand the Navier-Stokes equations. The computers can only do numerical approximations, and they have to come up with simplifications to be able to produce results within an acceptable time frame. All the approximations and simplifications that are made makes it impossible for the models to completely replicate what would happen in nature. One of the great challenges is to make sure that the imperfections are reasonably small, so the simulation results still are as close to reality as necessary. CFD has proven to be accurate enough for this type of simulations to get useful results, so CFD is the approach that has been chosen.

### 4.2. Software

The software in which the geometrical model was built, the simulations carried out, and the post processing performed, has been Ansys.

There are many commercial software that are able to do the same simulations as Ansys, so other programs can be used. Ansys has a good reputation for being user friendly and widely adopted, so for someone with limited prior experience with CFD software, it is relatively easy to start working with, both because of its user friendly design, but also for the amount of help that can be found on the Internet, e.g. tutorials on YouTube and fora where common problems are discussed. Another great advantage of Ansys is that everything can be done within the same software, from building the model of the burner to post processing, so transitions from different phases in the workflow are smooth and seamless.

### 4.3. Model of the Burner

This section contains a description of how the model of the burner was built, what geometrical proportions the model has, which simplifications that were made, and how the mesh was designed.

#### 4.3.1. Geometry

The geometry of the burner is based on the burner used by the School of Automotive Studies at Tongji University, but with simplification. The biggest simplification was to reduce the problem to only 2 dimensions. Fluid turbulent flow is always a three dimensional process, so reducing the problem to only two dimensions inevitably made the solutions less accurate. The burner is however completely

symmetric around its x-axis, so the penalty for reducing the problem to 2D is relatively mild. The advantage of reducing the problem with one dimension is to save computer power. Calculating in 3D would take too much time. Had 3D been used, only very few simulations could have been made within the time frame of this project, and that would not have been enough to be able to draw conclusions of how the flame behaves when conditions change. Ansys have special physical models that are used when working with 2D CFD, and reducing problems to 2D is common in the industry and in the academic world, so there are no reasons to believe that the reduction of this problem to 2D made the results non trustworthy due to that decision.

The model was also simplified by cutting it along its x-axis, which is also its symmetry axis. If the remaining piece made a rotation of 360 degrees around its x-axis, it would create the 3D representation of the burner. This simplification made the problem even less computational demanding since the model then was reduced in size with 50%. Ansys supports this simplification by a pre-setting in the software. Figure 6 shows how the model looks to scale. The white line in the centre is the x-axis and the model in the figure is reflected in this line to give a better representation of how the burner looks. Table 2 lists the most important dimensions and the complete set of the measurements can be found in the Appendix.

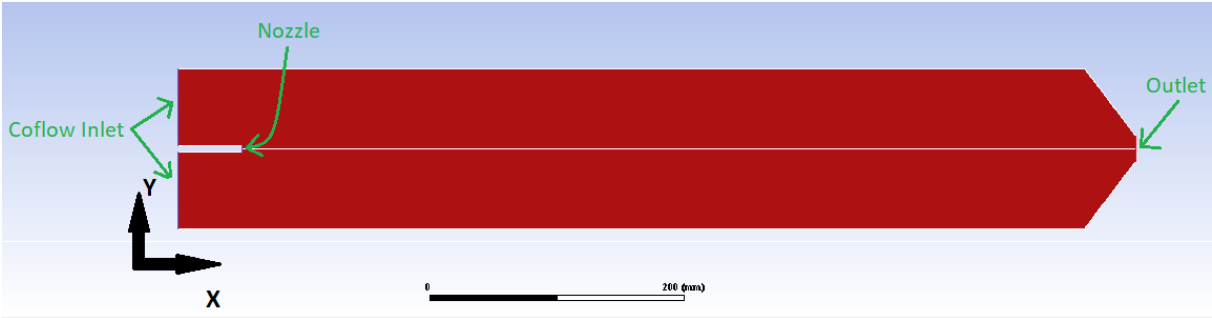


Figure 6. The model of the burner.

Table 2. The most important measurements of the burner.

Dimensions	[mm]
Nozzle diameter	4.6
Coflow inlet diameter	125
Distance between the nozzle and the outlet	700
Distance between the coflow inlet and the nozzle	50

4.3.2. Mesh

Constructing a good mesh is a process full of compromises. Only considering getting accurate solutions, the cells should be as small and many as possible. The cost of more cells are however an increase in computational time required to get a solution. There is a trade-off between time and accuracy, and both must be taken into consideration when constructing the mesh. Some tricks can be used to get time efficient and accurate results: As mentioned earlier, reducing the problem to 2D, and further cutting it in half saves a huge amount of cells, and therefore also time. Another trick is to have small cells in interesting areas (refinement zones) such as where the combustion takes place, where huge turbulence is expected, around small edges, and where gradients in pressure, velocities, temperature, etc. are expected. A refinement zone was created along the x-axis, stretching out halfway to the walls. Simulations later showed that the flame and the flow in different cases varied a lot with different

conditions, so the refinement zone would have to be expanded so much that it mostly covered the whole burner. Due to these findings, that refinement zone was abandoned and all cells in the chamber were set to the same size except for the cells closest to the nozzle. Quadrilateral cells are generally the best cell shape to use in 2D problems (Bommes, Lévy, Pietroni, Puppo, & Silva, 2012), so it is what has been used here. The element size in the mesh closest to the jet inlet is 0.2\*0.2 millimetre and for the rest of the area the cells are 1\*1 millimetre (the cells in the transition areas are somewhere in-between these sizes). Figure 7 shows the cell structure around the nozzle. The model contains 43 000 cells in total.

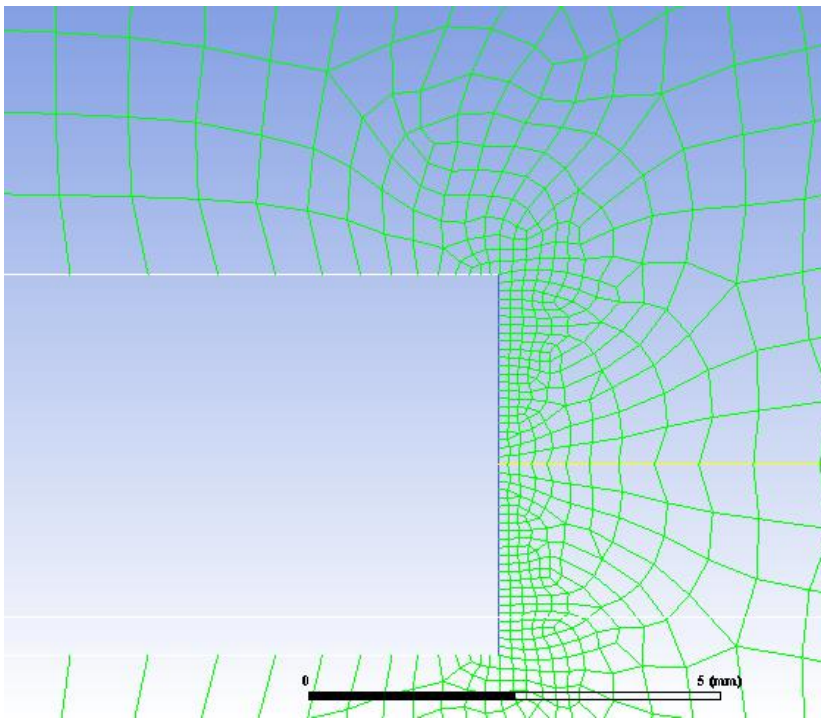


Figure 7. The mesh around the jet inlet.

#### 4.4. Setup

To be able to start the simulations, boundary conditions and models have to be chosen. The models that have been used have already been presented under *Theory*, where the underlying equations and assumptions are presented. Under this section justifications to why the models were chosen will be presented. The boundary conditions of the burner is also presented.

##### 4.4.1. Boundary Conditions

Many parameters were intentionally set to match those used in the famous paper from Cabra et al. (2005) that is referred to under *Previous Findings*. Their burner shares many similarities with this one, and keeping similar boundary conditions will make a comparison of the results relevant and differences in the results are easier to understand when just a few parameters differ. The base condition for the methane case is a temperature of 1350 K for the coflow and 320 K for the fuel. The velocities are 4.2 m/s and 100 m/s respectively. The base condition for the hydrogen case is a temperature of 1045 K for the coflow and 305 K for the fuel. The velocities are 3.5 m/s and 107 m/s respectively. The base coflow velocity for the methane case is a little bit different from the one used in the paper from Cabra et al. (2005), this is because 4.2 m/s is a velocity that is more relevant for the team at Tongji University. The rest of the velocities, and all of the temperatures are however the exact same and these parameters are also within the interval which the burner in Tongji University is planned to be operated at. The composition of the jet- and coflow gases are almost the same as the compositions used in the paper

from 2005, but there are a few minor differences. Table 3 list the boundary conditions and the composition of the gases for the base-scenario. Compare with Table 1 to see differences and similarities between the values used in this study and the ones used by Cabra et al. (2005).

Table 3. Base-case conditions for the burner. Conditions for both the hydrogen and the methane cases are listed. *d*, nozzle diameter; *V*, velocity; *T*, temperature; *X*, mole fraction.

	Hydrogen		Methane	
	Jet	Coflow	Jet	Coflow
<i>d</i> (mm)	4.6	125	4.6	125
<i>V</i> (m/s)	107	3.5	100	4.2
<i>T</i> (K)	305	1045	320	1350
$X_{O_2}$	0.0021	0.15	0.15	0.12
$X_{N_2}$	0.7464	0.751	0.52	0.73
$X_{H_2O}$	0.0015	0.099	0	0.15
$X_{OH}$ (ppm)	0	0	0	0
$X_{H_2}$	0.25	0	0	0
$X_{NO}$ (ppm)	0	0	0	0
$X_{CH_4}$	0	0	0.33	0

The purpose of this project is to test the burner for different conditions, and those conditions differ depending on what fuel is being used. For methane, different velocities of the coflow and jet were tested. What velocities are feasible is hard to guess, so previous experience and others experiment comes in handy to get a reference point of what has worked before. The conditions used in this project have mainly been inspired by the experiments from Cabra et al. (2005). Mimicking their conditions will also make it easy to compare the results plotted in Figure 2 and Figure 3. The cases tested for methane have a coflow velocity set to 4.2 m/s while the jet velocity was set to [25; 50; 75; 100; 150; 200] m/s and coflow velocities set to [4.2; 5.3; 6.5] m/s while the jet velocity was fixed at 100 m/s.

For hydrogen, different pressures and jet velocities were tested. Cabra et al. (2005) used an open burner, thus they only tested for atmospheric pressure. The approach to decide which pressures to use was simply trial and error since this specific set up was new to the team and little guidance were found in previous research. When the pressure was set too high, the flame was blown out. Different pressures were tested to see where these limits are and pressures in between atmospheric pressure and the limit were tested to look for trends of how the flame behave. The aim was first to only let the pressure vary, but the outcome of the simulations were a little surprising, so it was decided that different pressures also should be tested for jet velocities of 50 and 25 m/s as well. When the jet velocity was set to 107 m/s, the pressure started at 1.00 bar and was increased by 0.05 bar until it was blown out. To speed up the process for the cases with jet velocities of 50 and 25 m/s, the resolution was reduced at the lower pressures and the pressures tested were [1.00; 1.10; 1.25; 1.35; 1.40; 1.45] m/s. Higher resolution was applied close to the blow out limit.

#### 4.4.2. Models

CFD is full of models that approximates nature. Simplifications are necessary to keep simulation time down. Since the models cannot completely predict the results of the real world, they all have their advantages and disadvantages. When choosing what model that should be used, there are a lot of

things to take into consideration, such as what kind of experiment that is simulated and for how long the simulations can run. Many of the settings in Ansys have been kept unchanged. The main active choices of models and settings will be presented here.

#### *Gravity*

Gravity has been turned off. Turning off the gravity saves computational power, and it is not expected to influence the simulation notably. The chamber is less than one metre high, and the flow is several metres per seconds, so natural-convection will be very small since the gas is spending such a short amount of time in the chamber. The pressure difference between the top and the bottom due to gravity is also negligible.

#### *Turbulence Model*

The turbulence model that was chosen was the standard  $k-\epsilon$  model. This model is one of the most popular models to use in simulations that mainly consist of turbulent flow. It is widely known for its robustness, economy and reasonable accuracy for a wide range of turbulent flows (Ansys, 2006). The flow in the chamber is always turbulent (except close to the walls), so the conditions fit the strengths of the model.

#### *Chemistry Model*

For the chemical reactions, the composition PDF transport model was chosen. The model is considered to be very accurate, but also very slow. Since the problem was set to 2D and with relatively few cells, it was possible to implement the model without getting too slow simulations. This model was however by far the most time contributing factor in the simulations. When another, more simple, chemical model was tested, the simulation time was around 30 minutes, but with the composition PDF transport model, the simulation time rose to around 30 hours. The results from the simulations were however very different when changing to the simpler model, so it was clear that the gain in accuracy was worth the higher price in simulation time.

#### *Mixing Model*

There are three different mixing models to choose from in Ansys when the composition PDF transport model is activated. Cobra et. al. (2005) tested all of these available models when simulating lifted flames in hot coflow. They compared the simulations with laboratory experiments and they found that the model that best predicted reality was the modified Curl model. Based on that founding of the paper, it was decided that the modified Curl model would be used.

#### *Radiation Model*

Radiation is not expected to have a huge effect of the end result of the simulations, but in some research the radiation was included when simulating similar scenarios. Simulating radiation does not require a lot of computational power for the models used, so it was decided to include radiation in the simulations. The P-1 model has been used in previous research, so that is the one that has been used in this project. The P-1 model's main disadvantage is that it works poorly with optically thin media and that it assumes all surfaces to be diffuse. The gas in the chamber is optically thin, so it is not expected to predict the radiation effect on the gas perfectly. However, the wall of the gas chamber has a matte finish, so it is not considered to be a problem that the model assumes it to be completely diffuse.

## 5. Results

In this section, the results from the simulations will be presented, starting with the methane cases and then the hydrogen case. Comparisons with previous research will be made when applicable.

### 5.1. Methane

The results from the simulations with methane as fuel will be presented under this section. The influence of the coflow velocity is first presented and compared to the results from Cabra et. al. (2005), then the influence of the jet velocity is presented.

#### 5.1.1. Coflow velocity

The liftoff height divided by the nozzle diameter ( $H/d$ ) in the base scenario for the methane case ( $V_{jet} = 100$  m/s and  $V_{coflow} = 5.4$  m/s) is 26. The liftoff height is however dependent of both coflow velocity as well as jet velocity, so the liftoff height vary with different conditions. Figure 8 shows how the liftoff height vary with different coflow velocities. The relationship seems to be linear, but the influence of the coflow velocity seems to be small. The liftoff height goes from  $H/d = 24$  to  $H/d = 27$  when the jet velocity goes from 4.2 to 6.5 m/s.

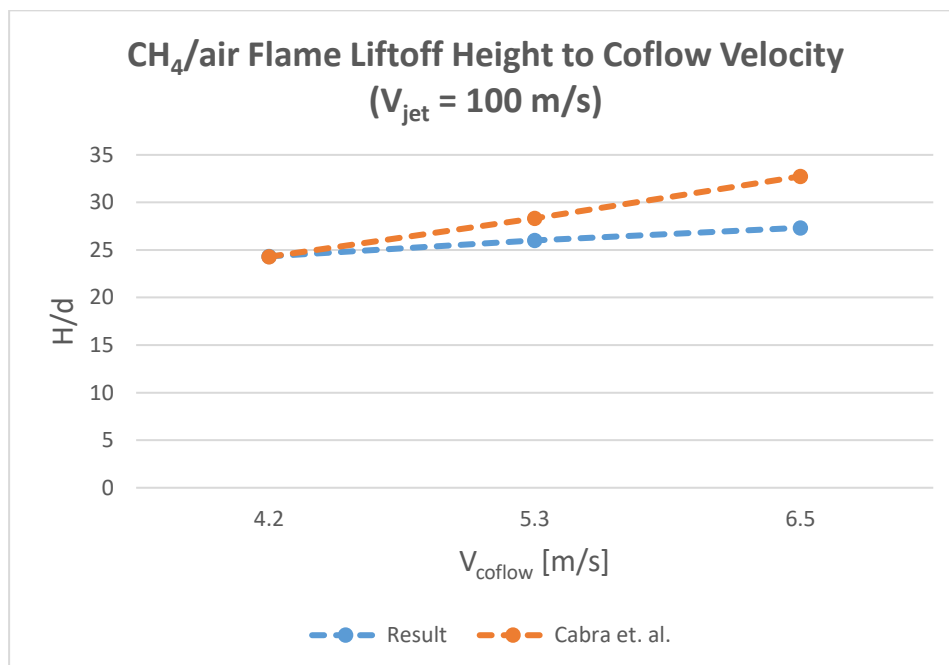


Figure 8. Sensitivity of methane flame liftoff height to coflow velocity. Jet exit velocity is constant at 100 m/s.

There are only three different data points, so more data points could have given a more detailed picture of how the liftoff height vary, but the general trend, that the liftoff height increase with increased coflow velocity, would probably not change with more data points. Previous research from Cabra et al. (2005), shows a very similar trend where the liftoff height is linearly increasing with higher coflow velocity. Their results have been included in Figure 8 to make the comparison of the results easy.

Figure 9 shows the temperature and OH mass fraction fields for different coflow velocities. The OH mass fraction is a good indication of where combustion takes place (Cabra, 2003). As can be seen, the combustion seems fairly similar for all three cases, but some minor differences can be seen. At the two lower velocities, some combustion is taking place near the chamber exit. At  $V_{coflow} 6.5$  m/s, the flame is shorter and also narrower. Since higher coflow velocity makes the combustion leaner, it is expected that the area close to the walls will be dominated by non-reacting gas.

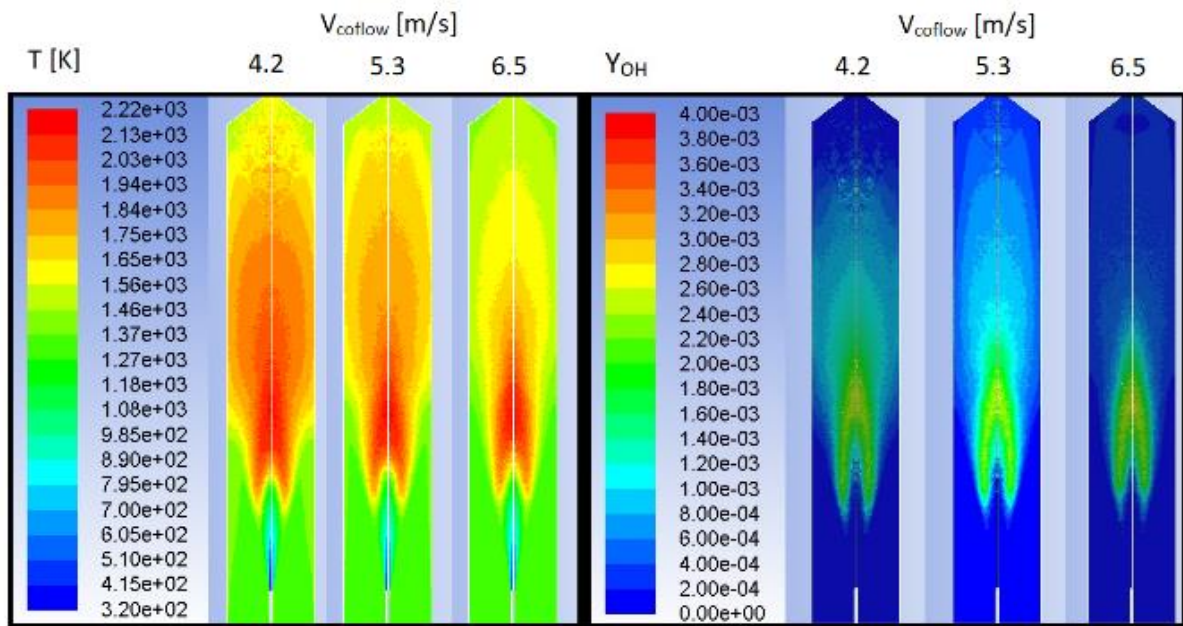


Figure 9. The temperature and OH mass fraction fields for different coflow velocities for the methane cases.

### 5.1.2. Jet Velocity

From Figure 10 we can see that the liftoff height relation to jet velocity is more complex compared to the relation to coflow velocity. When  $V_{jet}$  is doubled from 25 to 50 m/s, the liftoff height also doubles and goes from  $H/d = 10$  to  $H/d = 20$ . When  $V_{jet}$  increase beyond 50 m/s, the liftoff height becomes less sensitive, with the transition taking part when  $V_{jet}$  is between 50-100 m/s. The sensitivity seems to have stabilized for velocities over 100 m/s.

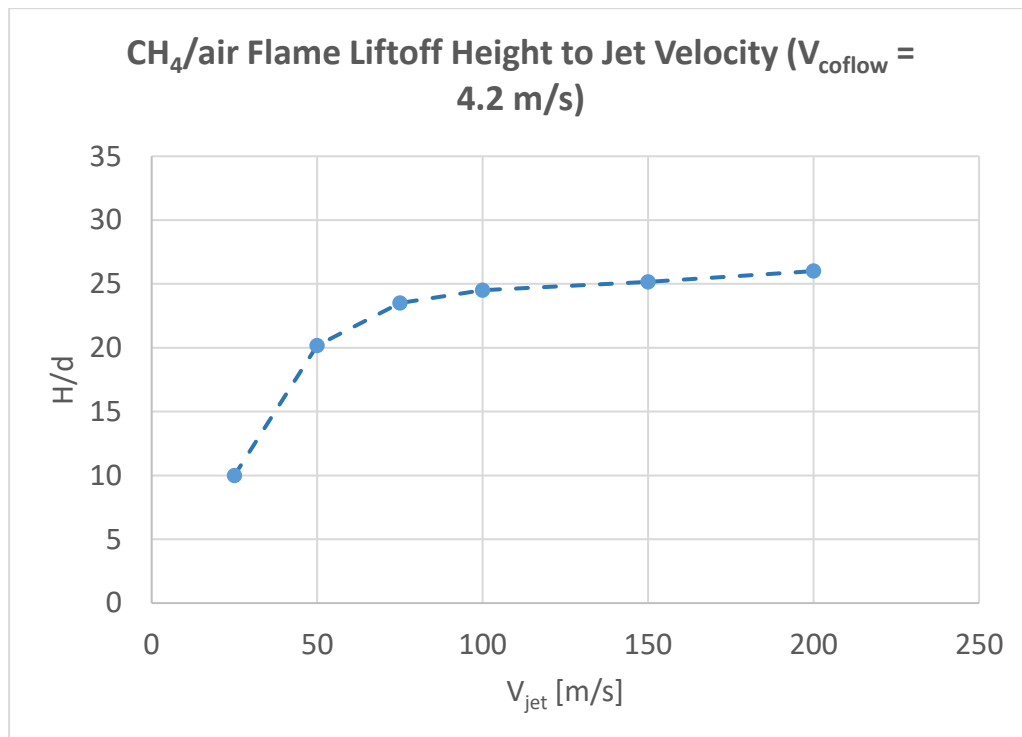


Figure 10. Sensitivity of methane flame liftoff height to jet exit velocity. Coflow exit velocity is constant at 4.2 m/s.

A closer look on the simulations helps to explain the curve. Figure 11 shows the temperature and the OH mass fractions fields for different jet velocities. When  $V_{\text{jet}}$  is only 25 m/s, the flame is on the verge of being attached. However, when looking closely it is possible to see that flame is indeed not attached. The flame is very thin and relatively long, so it is hard to determine exactly where the flame begins, so the said liftoff height of  $H/d = 10$  should be taken as a rough estimation. What the simulation more clearly suggest is that a  $V_{\text{jet}}$  of 25 m/s is somewhere in the transition between attached flame and liftoff flame.

When  $V_{\text{jet}}$  is higher, around 50 to 100 m/s, the flame does not change much, but there are big differences between  $V_{\text{jet}}$  100, 150 and 200 m/s. At  $V_{\text{jet}}$  100 m/s, we can see that the flame is starting to expand in width in the second half up streams of the chamber. The flame when  $V_{\text{jet}}$  is 150 m/s has expanded all the way out to the walls and the combustion has reached the very end of the chamber. The flame at  $V_{\text{jet}}$  200 m/s has a completely new shape: the combustion is no longer mainly in the centre, but has shifted and is now most intense in a ring around the centre jet stream. The reason for this behaviour can be found when looking at the aerodynamics.

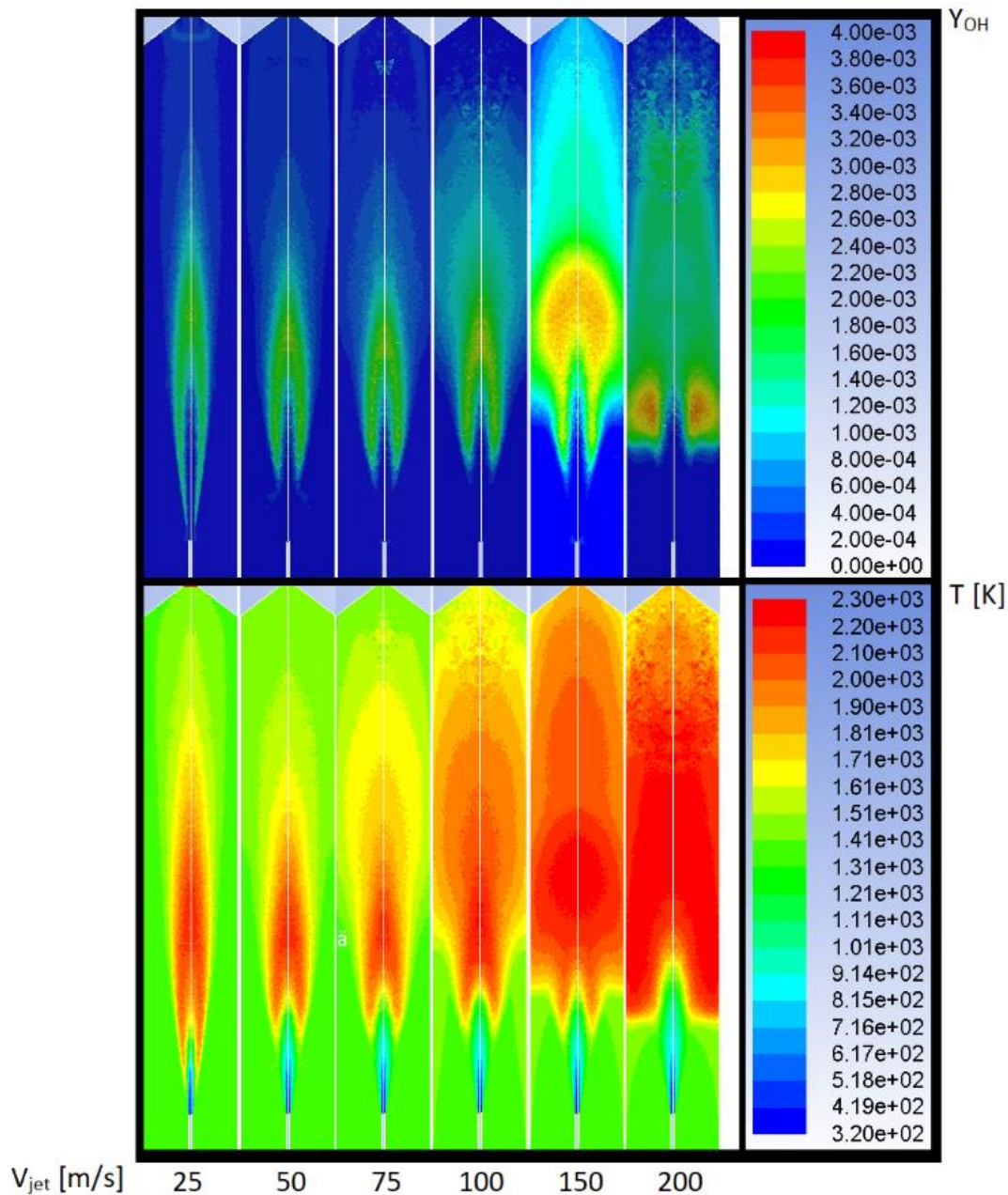


Figure 11. The temperature and OH mass fraction fields for different jet velocities for the methane cases. Coflow exit velocity is constant at 4.2 m/s.

Figure 12 shows the velocity vectors for  $V_{jet}$  100 and 200 m/s. At  $V_{jet}$  200 m/s there is a clear zone of recirculation that occurs in the lower third of the chamber. This zone is starting to form at  $V_{jet}$  100 m/s, and at even lower jet velocities the velocity vectors are mainly completely straight. The recirculation zone is at the same place as where the main combustion is taking place (seen in Figure 11), and it is plausible that this zone highly influence the shape of the flame.

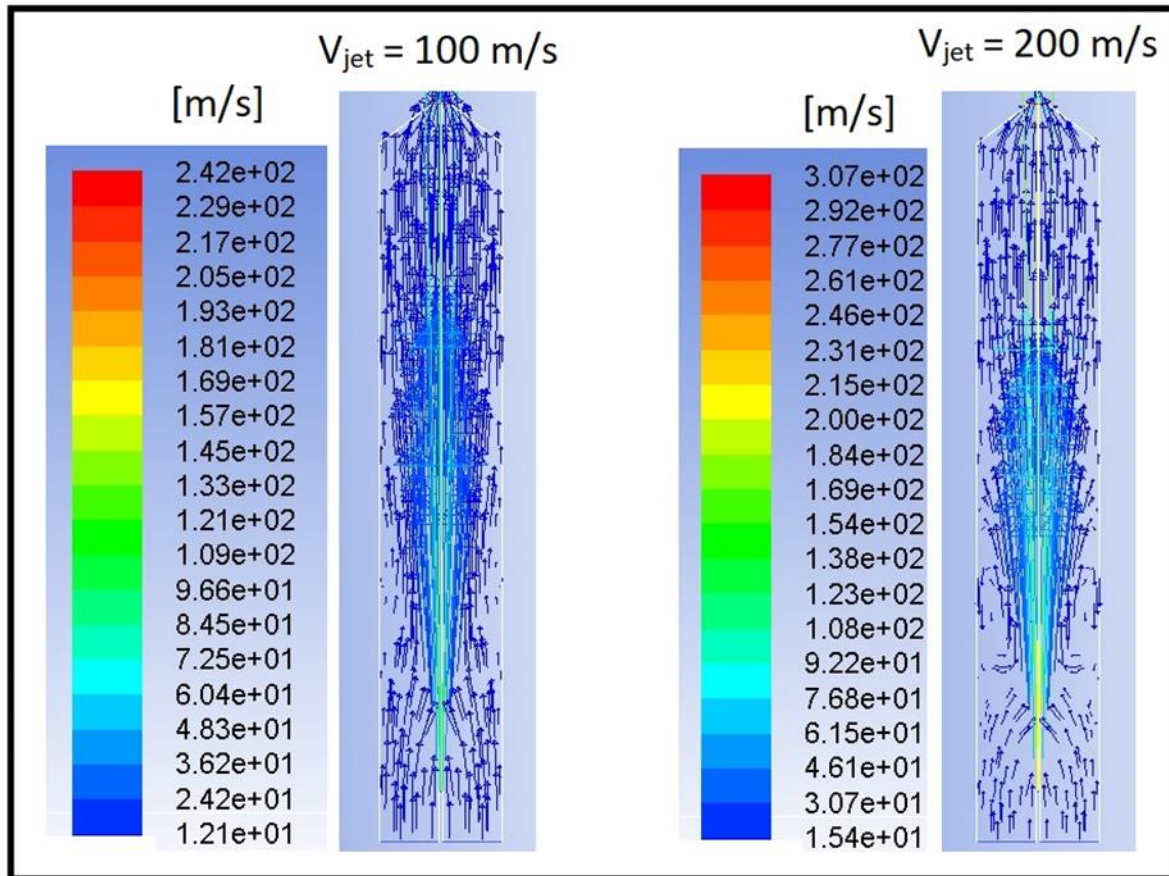


Figure 12. Velocity vectors for the gas flow for the methane cases. Note the recirculation area that is starting to form at  $V_{jet}$  100 m/s and that is fully developed at the  $V_{jet}$  200 m/s.

## 5.2. Hydrogen

For the hydrogen cases, all simulations were done with the same coflow velocity (3.5 m/s), but different jet velocities in combination with different background pressures were used. Figure 13 shows the liftoff height for different jet velocities and pressures. The trends in these environments are not very clear, but some patterns are however possible to extract. A general property seems to be that the liftoff height is very sensitive to changes in background pressures. The simulations did eventually converge, so according to the software the flames seemed stable at each test, but comparing the liftoff height from slightly different background pressures, it is reasonable to suspect that the liftoff heights might be unstable and hard to predict prior to laboratory experiments. For example, at  $V_{jet}$  107 m/s, the liftoff height changes from  $H/d$  15 to  $H/d$  29 when the pressure changes from 1.10 to 1.15 bar. That is a very big change in liftoff height for a very slight change in pressure. There is no clear trend of what happens when the pressure goes from atmospheric pressure to 1.10 bar when comparing the different jet velocities with each other. The liftoff height for  $V_{jet}$  107 m/s and  $V_{jet}$  25 m/s declines while it increases for the  $V_{jet}$  50 m/s case. What happens after 1.10 bar is however more consistent, all of the cases show a dramatic increase in liftoff height until they finally blow out.

Another trend seems to be that the slower the jet velocity is, the more background pressure the flame can withstand before it is blown out, and the higher up in the chamber the blow out point is.

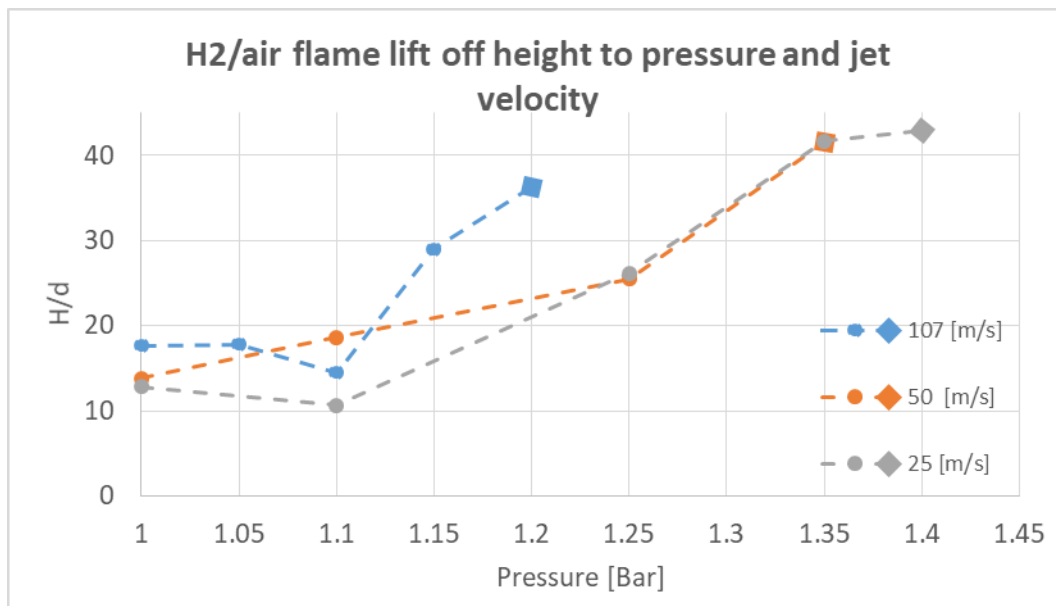


Figure 13. The liftoff height for different jet velocities for hydrogen flames. The last data point for each jet velocity is the highest pressure where there still is a flame. Coflow velocity is constant at 3.5 m/s.

Figure 14 shows the temperature and OH mass fraction for different background pressures at a jet velocity of 107 m/s. As can be seen, the flame seems to be relatively stable when it comes to power when the background pressure varies between 1.00 bar and 1.10 bar. Pressure above that level produce weak flames and as the flame is getting weaker, the liftoff height increases. The flame is so weak at 1.15 to 1.20 bar that most of the fuel never ignites. At pressures above 1.20 bar the flame is completely gone. Looking at the velocity vectors does not give any hint of why the flame is so sensitive. The flow is practically the same regardless of background pressure. The vectors look nearly identical as the one for  $V_{jet}$  100 m/s in Figure 12.

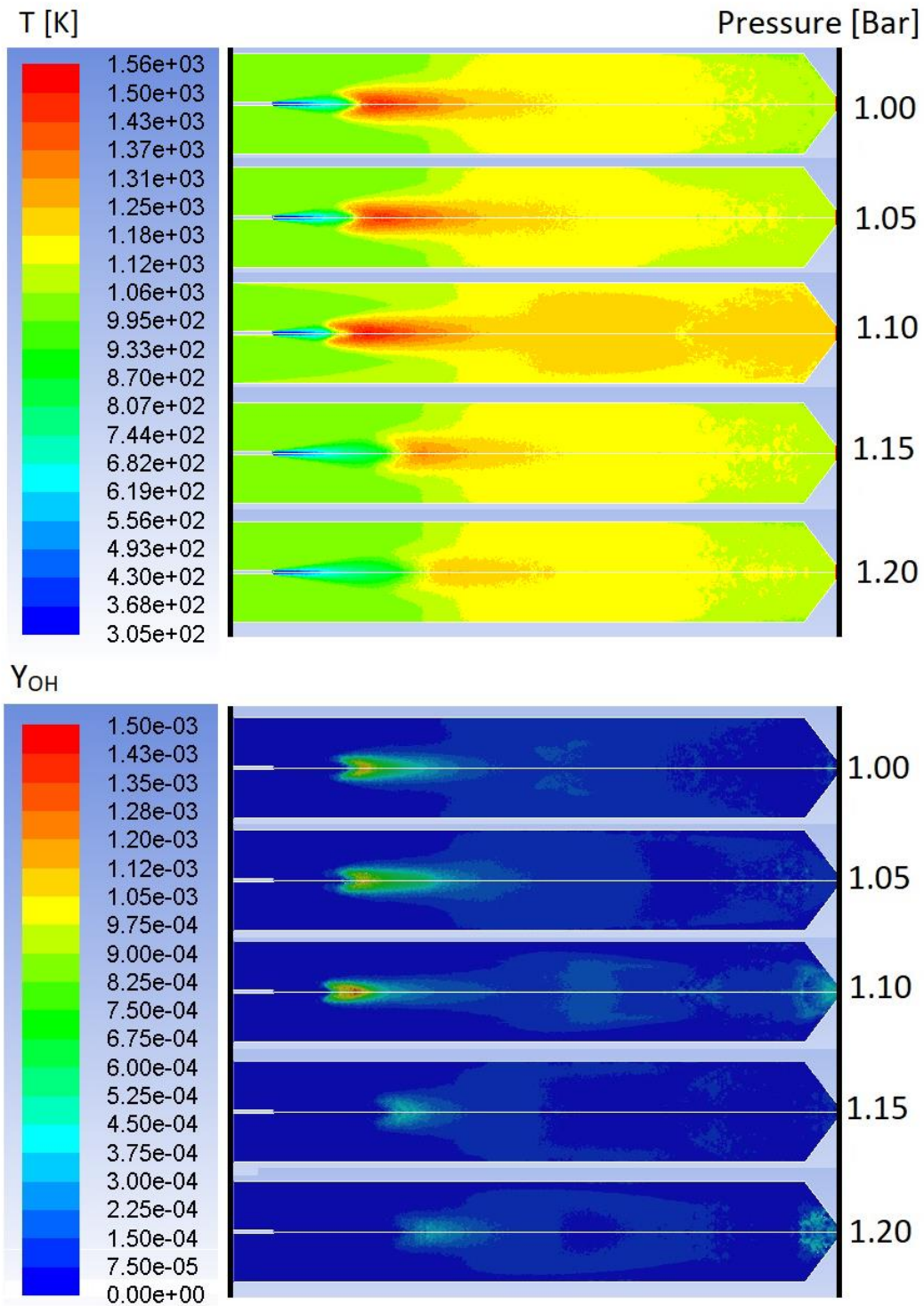


Figure 14. The temperature and OH mass fraction for different background pressures at a jet velocity of 107 m/s for the hydrogen cases.

## 6. Discussion

Research on lifted jet flames is important to gain further knowledge about how the flames behave in different conditions and how different parameters influence the flame. With enough knowledge it is possible to construct burners with very efficient flames. The research in this field has been ongoing for decades and there are still a lot of things that are unknown. Research with the help of simulations has been growing in popularity, mainly due to more powerful computers. When simulations have been compared to laboratory experiments, the results of the simulations have proven to be fairly close to the reality, especially when looking at different trends in the flames behavior. The study from Cabra et. al. (2005) compared simulations with experiments, and the simulations proved to predict reality quite accurately. The set up that they used is very similar to the one that has been used in this report, but the main difference is that the study by Cabra et. al. (2005) was on open burners while the one in this paper is on a closed chamber. Beside that difference, conditions have intentionally been the same, or almost the same as the ones used in the study by Cabra et. al. (2005).

The results from the methane case in this study were mostly as expected. The general trend of having higher liftoff when the coflow and jet velocity increased has been reported in many studies. The results from the methane case with increasingly fast coflow was well in line with previous research, but the liftoff height was a bit less sensible to coflow velocity than Cabra et. al. (2005) had experienced. When it comes to the relationship between liftoff height and jet velocity, the general trend with higher liftoff for higher jet velocity was expected and achieved. At low jet velocities ( $V_{jet}$  ranging from 25 to 75 m/s) the trend were linear and very steep, much steeper than Cabra et. al. (2005) achieved. When the jet velocity increased from 100 m/s and above, the aerodynamics of the burner started to play a major role in how the flame behaved. The recirculation zone (seen in Figure 12) is a direct consequence of having a chamber, so this effect cannot be seen in open burners. To control the recirculation zone, the aerodynamics of the chamber has to be thoroughly analyzed.

When it comes to the hydrogen cases, the liftoff height was lower in the base scenario compared to the methane base scenario. This was expected and in line with previous research. What was surprising, however, is that the flame is incredibly sensitive to changes in background pressure. As small changes as 0.05 bar gave huge changes in liftoff height. The low blow out limit also came as a surprise. The flames started out with a lower liftoff height when the jet velocity was lower, which was expected. The flame could also withstand higher pressure the lower the jet velocity was. An explanation to the mechanism behind the high sensitivity to pressure and why the flames blow out at relatively low pressures is desired, but no satisfying reason could be found by in this study. Further research on the behavior of flames in high pressure and of the mechanisms is suggested.

Where applicable, the results in this study were in line with the findings from Cabra et. al. (2005), which set ups are similar to the ones in this study. This suggest that the results from the simulations in this study are realistic also in the range where comparisons have not been possible.

Simulations are however just numerical approximations of simplified models of complex phenomena, so results from simulations should not automatically be seen as the truth. Especially not before experiments can confirm the results. None of the results in this thesis have been tested in Tongji University's chamber, so they have not yet been confirmed. If the laboratory experiments are conducted and the results are in line with the results of the simulations, the credibility of the other results rises.

## 6.1. Relevance to the Automotive Industry

Hydrogen and methane are fuels that are used in commercial cars today, but the market shares of those cars are very small. Even though there has not been a big commercial breakthrough yet, there is still research in the automotive industry on these fuels. The methods that have been used in this project are general, and they can be applied on four-stroke engines, which are more conventional in the automotive industry.

## 7. Conclusion

When it comes to the methane cases, the liftoff height is growing with increasing coflow velocity. The relationship is however weak, so a large increase of the coflow velocity will only give a small increase of the liftoff height. When it comes to jet velocity, 50 to 100 m/s seems to be the best range. With slower velocities than 50 m/s, the liftoff height is decreasing rapidly and the flame is about to become attached. With higher velocities than 100 m/s, the combustion is getting very rich, and a recirculation zone in the chamber is beginning to show, which makes the flame change shape. The main combustion goes from being located centered above the nozzle to being located in a ring above the nozzle.

When hydrogen is used as fuel, the flame is very sensitive to changes in pressure, but the lower the jet velocity is, the higher pressure the flame can withstand before it is blown out. At pressures above 1.10 bar, the liftoff height of the flame drastically increase and its temperature drastically decrease. There is no clear trend of how the flames behave when the pressure goes from 1.00 to 1.10.

When comparable, the results are in line with previous research, which indicates that all results are realistic. However, it is not possible to be certain before laboratory experiments can confirm the results that have not been able to be compared with previous research.

## 8. Recommendations and Suggestions for Further Work

A recommendation to the team at Tongji University is to use a jet velocity in the interval of 50-100 m/s to achieve a flame that has a stable liftoff height and that is neither too lean nor too rich when methane is being used as fuel.

To redesign the chamber to get rid of the recirculating zone that occurs in high jet velocities, if that is seen as a problem that is, might be a big project. Further investigation of how this should be achieved, and how the results will change with such change, should be done before such a big decision is taken.

The hydrogen flame is very sensitive to changes in background pressures, so a precise control of the pressure is needed to be able to run it efficiently. Since the flame is so sensitive, and because it is easily blown out, the team at Tongji University should further investigate how different temperatures and gas mixtures affect the combustion. Increasing the temperature might be an easy way to increase the blow out pressure and to make the flame more stable.

## 9. Bibliography

- [1] Lumley, J.L., SpringerLink Archive (e-book collection) & SpringerLink (e-book collection) 1990, *Whither turbulence?: turbulence at the crossroads : proceedings of a workshop held at Cornell University, Ithaca, NY, March 22-24, 1989*, Springer-Verlag, New York;Berlin;.
- [2] Westerweel, J., Boersma, B.J., Nieuwstadt, F.T.M., SpringerLink (Online service) & SpringerLink (e-book collection) 2016, *Turbulence: Introduction to Theory and Applications of Turbulent Flows*, Springer International Publishing, Cham.
- [3] White, F.M. 2011, *Fluid mechanics, 7th in SI units edn*, McGraw-Hill, Singapore.
- [4] Ansys, *Ansys Fluent User's Guide*. (2006), New York: Fluent Inc.
- [5] Warnatz, J., Maas, U., Dibble, R.W. & SpringerLink (e-book collection) 2006, *Combustion: physical and chemical fundamentals, modeling and simulation, experiments, pollutant formation*, 4th edn, Springer, New York;Berlin;
- [6] McAllister, S., Chen, J., Fernandez-Pello, A.C. & SpringerLink (e-book collection) 2011, *Fundamentals of combustion processes*, Springer, New York
- [7] Turns, S. R. (2006). *An Introduction to Combustion*. Mc
- [8] Mansour, M.S. 2003, "Stability characteristics of lifted turbulent partially premixed jet flames", *Combustion and Flame*, vol. 133, no. 3, pp. 263-274.
- [9] Navarro-Martinez, S. & Kronenburg, A. 2011, "Flame Stabilization Mechanisms in Lifted Flames", *Flow, Turbulence and Combustion*, vol. 87, no. 2, pp. 377-406.
- [10] Tacke, M.M., Geyer, D., Hassel, E.P. & Janicka, J. 1998, "A detailed investigation of the stabilization point of lifted turbulent diffusion flames", *Symposium (International) on Combustion*, vol. 27, no. 1, pp. 1157-1165.
- [11] Leung, T. & Wierzba, I. 2009, "The effect of co-flow stream velocity on turbulent non-premixed jet flame stability", *Proceedings of the Combustion Institute*, vol. 32, no. 2, pp. 1671-1678.
- [12] Cabra, R., Chen, J.-., Dibble, R.W., Karpetis, A.N. & Barlow, R.S. 2005, "Lifted methane-air jet flames in a vitiated coflow", *Combustion and Flame*, vol. 143, no. 4, pp. 491-506.
- [13] Senouci, M., Benchatti, T., Bounif, A., Oumrani, N.O. & Merouane, H. 2016, "A hybrid rans-rsm/composition pdf-transport method for simulation of hydrgen-air turbulent diffusion flame", *International Journal of Heat and Technology*, vol. 34, no. 2, pp. 268-274.
- [14] Meyer, D.W. & Jenny, P. 2013, "Accurate and computationally efficient mixing models for the simulation of turbulent mixing with PDF methods", *Journal of Computational Physics*, vol. 247, pp. 192-207.
- [15] Krishnamoorthy, G. 2017, "A computationally efficient P-1 radiation model for modern combustion systems utilizing pre-conditioned conjugate gradient methods", *APPLIED THERMAL ENGINEERING*, vol. 119, pp. 197-206.
- [16] Cintolesi, C., Nilsson, H., Petronio, A. & Armenio, V. 2017, "Numerical simulation of conjugate heat transfer and surface radiative heat transfer using the P1 thermal radiation model: Parametric study in benchmark cases", *International Journal of Heat and Mass Transfer*, vol. 107, pp. 956-971.

- [17] Wilcox, D.C. 2006, *Turbulence modeling for CFD*, 3rd edn, DCW Industries, La Cãnada, Calif.
- [18] Bommès, D., Lévy, B., Pietroni, N., Puppo, E., Silva, C. 2012, "State of the Art in Quad Meshing", *Eurographics STARS*.
- [19] Cabra, R. 2003, *Turbulent jet flames into a vitiated coflow*, ProQuest Dissertations Publishing.

# Appendix

The complete set of the burner's measurements

